JOURNAL OF CATALYSIS 62, 329–340 (1980)

Decomposition of Methyl Formate on W(100), W(100)–(5 × 1)C, and W(100)–CO(β) Surfaces

M. A. BARTEAU AND R. J. MADIX

Department of Chemical Engineering, Stanford University, Stanford, California 94305

Received May 1, 1979; revised September 13, 1979

The decomposition of methyl formate was examined using temperature-programmed reaction spectroscopy under ultrahigh vacuum conditions on single-crystal W(100), W(100)–CO(β), and W(100)–(5 × 1)C surfaces. The W(100) surface was highly selective toward formation of CO(β) and hydrogen from methyl formate. Hydrocarbon species, including methane, were produced on this surface from a complex with a stoichiometric excess of hydrogen only after the CO(β) states were saturated by cracking methyl formate. Passivation of the surface by adsorption of CO to form the W(100)–CO(β) surface prior to exposure to $HCOOCH_3$ shifted the selectivity in favor of H_2CO and CH_3OH. Methyl formate decomposition on this surface followed a reaction pathway different from that on the W(100) surface: no hydrogen-excess surface complex was formed, and no methane was produced on the W(100)–CO(β) surface. Passivation of the surface by formation of the carbide chemilayer also shifted the selectivity toward hydrocarbon formation. The reaction pathways observed on the W(100) and W(100)–CO(β) surfaces both took place on the W(100)–(5 × 1)C surface, and methane was again evolved as on the W(100) surface via a complex involving an excess of hydrogen. This unusual complex appears to involve multiple methoxy groups and surface tungsten atoms which stabilize the excess hydrogen.

INTRODUCTION

Much attention has been devoted over the past two decades to the study of adsorption and desorption phenomena on tungsten surfaces. Many of these studies have been concerned with the surprisingly complex behavior of simple probe molecules on these surfaces. For example, numerous workers have examined the adsorption of CO on a variety of single-crystal and polycrystalline tungsten surfaces. No fewer than six binding states for CO have been observed on the W(100) surface. These have been characterized as follows: the "virgin" state, formed by adsorption below 100 K, for which it has been proposed that the CO is bridge bonded between two tungsten atoms (*1*); the α_1 and α_2 states, in which each CO molecule is bonded linearly to a single tungsten atom (*2*); and the β_1, β_2, and β_3 states in which CO is dissociated into carbon and oxygen atoms which occupy adjacent four-fold sites on the surface (*3*). The origin of the multiplicity of the α and β states remains unresolved, although these effects have been attributed to lateral interactions between the adsorbed species (*3*). Likewise, the adsorption of H_2 has been studied by several workers. On the W(100) surface, hydrogen is adsorbed in two binding states, β_1 and β_2, which exhibit first- and second-order kinetics, respectively (*4, 5*). Several models (*5–7*) have been proposed for the structure of the hydrogen adsorbed on this surface; however, this question also remains unresolved.

In spite of the incomplete understanding of these simple systems, more complex systems can be profitably studied. The interaction of H_2 and CO, in particular, has been examined with a view toward determination of the properties of tungsten surfaces for methanation reactions. Several workers (*8–11*) have reported a reduction of the binding energy of hydrogen upon adsorption of CO, resulting in the formation of a new binding state, designated ν, for H_2 and CO. Benziger and Madix (*11*) reported that methane was evolved simultaneously

0021-9517/80/040329-11$02.00/0

with $CO(\nu)$ and $H_2(\nu)$ and suggested that these products result from a CO–hydrogen complex on the surface. The structure and composition of this complex, however, remain unresolved.

Decomposition reactions of hydrocarbon species have also been examined on clean and modified surfaces in order to determine the intermediate species involved in hydrocarbon formation and decomposition. Yates *et al.* examined the decomposition of H_2CO (*12*) and $HCOOCH_3$ (*13*) on the clean W(100) surface and reported the formation of CO, H_2, CH_4, and CO_2, as well as other hydrocarbon species. Based on the evolution of CH_4 and CO_2 at temperatures of 500 K and above, they suggested that the intermediate species in the production of CH_4 on the W(100) surface was $HCOOCH_3$. In a study directed toward understanding the surface reactivity of tungsten carbide, Ko, Benziger, and Madix examined the decomposition of CH_3OD (*14*) and H_2CO (*15*) on the W(100) and W(100)–(5 × 1)C surfaces. It was found that the selectivity for hydrocarbon formation increased substantially for both reactants on the W(100)–(5 × 1)C surface due to the suppression of the formation of $CO(\beta)$ by the surface carbon (*15*).

In the present study, we have examined the decomposition reactions of $HCOOCH_3$ on the W(100) and W(100)–(5 × 1)C surfaces in order to determine possible mechanisms for hydrocarbon production and to test the suggestion that $HCOOCH_3$ may act as an intermediate for the production of CH_4 from species such as CH_3OH and H_2CO. In addition, the decomposition of $HCOOCH_3$ on the W(100)–$CO(\beta)$ surface was studied, as preadsorption of $CO(\beta)$ appears to passivate the tungsten surface toward further production of $CO(\beta)$ from hydrocarbon decomposition in a manner similar to carburization.

EXPERIMENTAL

The experimental apparatus has been described in detail elsewhere (*16*). In addition to the quadrupole mass spectrometer used for monitoring reaction products, the system contained four-grid LEED optics and a double-pass cylindrical mirror analyzer used for Auger electron spectroscopy (AES). LEED and AES were used to determine the structure and composition of the surface, respectively.

The W(100)–(5 × 1)C surface was prepared by cracking ethylene on the W(100) crystal surface as previously described (*16*). The sample was heated to 1500 K between successive experiments in order to desorb any accumulated surface oxygen as CO. Thus maintained, the W(100)–(5 × 1)C surface was found to be free of observable degradation as determined by LEED and AES for more than 20 adsorption–desorption experiments.

The W(100) surface was prepared by successively heating the sample to 1500 K at a background pressure of 3×10^{-8} Torr of oxygen for several minutes, pumping away the oxygen, and heating the sample to 2500 K to remove volatile tungsten oxides until no impurities were revealed by AES. The clean W(100) surface was found to rapidly chemisorb CO in the dissociated β states, and the sample was heated to 2500 K before each experiment to desorb it. The sample could be cooled from 1500 to 300 K in 70 ± 10 sec. At base pressures of 2×10^{-10} Torr, this cooling rate was sufficient to provide a clean surface, as evidenced by the surface reconstruction from the $p(1 \times 1)$ to the $c(2 \times 2)$ structure at 300 K described by Debe and King (*17*). The work described for the clean W(100) surface was performed under these conditions: the $CO(\beta)$ adsorbed on the surface before dosing with methyl formate did not exceed 2% of a monolayer as determined by AES. Temperatures below 300 K could be achieved only by increasing the time allowed for cooling of the sample, resulting in greater adsorption of CO from the background. As such adsorption was found to significantly affect the reaction selectivity of the W(100) surface, reaction studies for adsorption of

$HCOOCH_3$ below room temperature were not performed.

The W(100)–CO(β) surface was prepared by dosing a clean W(100) surface at 300 K with CO introduced directly onto the surface by means of a 22-gauge needle. The CO(β) coverage was determined from the relative intensities of the W(350) and C(271) Auger signals (*16*), and the surface was found to be saturated for exposures of CO at a background pressure of 2×10^{-8} Torr for 2 min. The sample was heated to 600 K before each experiment in order to remove CO(α). This surface was found to be free of degradation for more than 10 adsorption-desorption cycles.

Methyl formate was purified by prolonged pumping at 195 K in a dry ice-acetone bath until a constant vapor pressure of 600 μm was achieved. Samples to be dosed into the chamber were introduced into the stainless steel dosing line immediately before dosing, and pumped down to the desired pressure for dosing (usually 150 μm). The cracking pattern for methyl formate shown in Table 1 was thus easily reproduced, and degradation of the methyl formate to formaldehyde in the dosing lines was minimized. (Contact of methyl formate with the stainless-steel dosing line for periods exceeding 5 min resulted in larger m/e = 29 and 30 signals for the sample dosed into the chamber due to H_2CO formation.) Methyl formate was admitted to the vacuum system through a 22-gauge stainless-steel needle, which provided a collimated beam of molecules directed onto the front face of the tungsten sample.

TABLE 1

$HCOOCH_3$ Cracking Pattern

Mass	Relative intensity
15	30
28	19
29	68
30	11
31	100
32	40
60	30

After preparation of the surface, the flash desorption experiments were conducted as follows. The sample was cooled to 295 K and dosed with methyl formate. The sample was then turned toward the ionizer of the mass spectrometer and heated at a constant rate of 20 K/sec by means of a tungsten filament located behind the sample. The product desorption spectrum was obtained as a function of temperature by monitoring both the mass spectrometer signal and the output of the thermocouple attached to the sample. The desorption spectrum of each product was corrected for overlapping cracking fractions, and absolute coverages were determined from the corrected desorption spectra in the manner described by Ko *et al.* (*14*). Coverages of CO(β) were determined by AES as described by Benziger *et al.* (*16*).

RESULTS

W(100)

The major result of the decomposition of methyl formate on the W(100) surface was the formation of hydrogen and CO(β). Seventy-five percent of the adsorbed methyl formate reacted to form these two products, with H_2 displaced from the surface during the adsorption process. CO(β) was desorbed from the surface only by electron bombardment heating of the sample above 1000 K. All other products desorbed from the surface below 600 K and are shown in Fig. 1. Subsequent to saturation exposure of the surface to methyl formate at 295 K, $HCOOCH_3$ desorbed at 355 K; CO and H_2 were produced simultaneously at 390 K; CH_3OH, H_2CO, CH_4, H_2, H_2O, and CO were produced simultaneously near 500 K; and CO_2 and H_2 were produced above 560 K. The actual desorption spectra were corrected in Figs. 1, 3, and 5 to reflect relative mass spectrometer sensitivities, so that the area under each curve is proportional to the absolute coverage of that product. Abso-

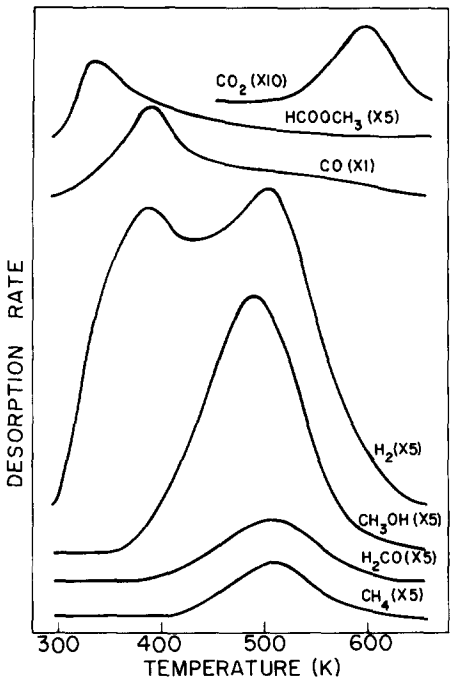

FIG. 1. Product desorption spectra for $HCOOCH_3$ adsorption on W(100): saturation exposure.

lute coverages for each of the products are listed in Table 2.

Coverage variation studies were also performed. At low exposures, CO(β) and H_2 were the only products observed. Other organic products were produced only after the CO(β) states approached saturation. With the exception of the $H_2(\beta_2)$ peak observed for low exposures, the peak temperatures of all of the products were found to be independent of coverage, so that all of these products resulted from first-order processes. Further, with the exception of methyl formate and CO(β), all of the products were observed above their desorption temperatures, indicating that their evolution was limited by reaction rather than by desorption.

The coverage and peak temperature of the unreacted methyl formate desorbed were found to be dependent upon the temperature at which the $HCOOCH_3$ was adsorbed. All other products were unaffected by the adsorption temperature. When ad-

TABLE 2

Product Distribution

T_d (K)	Product	Coverage (molecules/cm²)		
		W(100)	W(100)–CO(β)	W(100)–(5 × 1)C
355	$HCOOCH_3$	1.0×10^{13}	2.9×10^{13}	2.6×10^{13}
381–390	CO	6.0×10^{13}	7.4×10^{13}	1.4×10^{14}
390–408	H_2	4.4×10^{13}	2.4×10^{13}	3.8×10^{13}
408	CH_3OH		4.4×10^{13}	1.8×10^{13}
	H_2CO		3.8×10^{13}	1.1×10^{13}
471–500	CH_3OH	4.0×10^{13}		1.4×10^{13}
	H_2CO	9.6×10^{12}		1.1×10^{13}
	CH_4	7.3×10^{12}		2.8×10^{13}
	H_2	5.2×10^{13}		2.4×10^{13}
	CO	1.1×10^{13}		$<1 \times 10^{12}$
	H_2O	$<1 \times 10^{12}$		
560	CO_2	1.8×10^{12}	4.0×10^{12}	3.0×10^{12}
	H_2			1.6×10^{13}
Stoichiometry of desorbing products		CH_3O	$CH_{1.9}O$	$CH_2O_{.9}$
Adsorbed products				
	CO(β)	4.3×10^{14}		
	O(a)			3.0×10^{13}
Overall stoichiometry		$CH_{.75}O$	$CH_{1.9}O$	CH_2O
Total carbon adsorbed		5.8×10^{14}	2.2×10^{14}	2.8×10^{14}

sorbed at 295 K, $HCOOCH_3$ desorbed at 355 K. When adsorbed at 230 K, $HCOOCH_3$ desorbed at 285 K, with the resulting peak completely enveloping that observed for the 295 K adsorption. (See Fig. 2.) In addition, the $HCOOCH_3$ peak did not shift with coverage for a fixed adsorption temperature. Similar behavior was also observed on the W(100)–(5 × 1)C and W(100)–CO(β) surfaces.

The total product stoichiometry for saturation coverage of $HCOOCH_3$ was found to be $CH_{0.75}O$ by summing the coverages of products obtained by thermal desorption to the residual coverage of CO(β) remaining on the surface. This overall stoichiometry represented a hydrogen deficiency with respect to the parent molecule and indicated that hydrogen was displaced from the surface during the adsorption process. In contrast, the stoichiometry of the thermally desorbed products alone (i.e., excluding CO(β)) was CH_3O which represented a net excess of hydrogen with respect to the parent molecule, $HCOOCH_3$, suggesting that such surface methoxy groups were stable on the surface as intermediate species once the CO(β) states approached saturation. Further, the stoichiometry of products formed at 500 K was $CH_{4.5}O$, suggesting that surface complexes containing excess hydrogen were formed on the surface, as adsorbed hydrogen itself was not stable on the surface at this temperature.

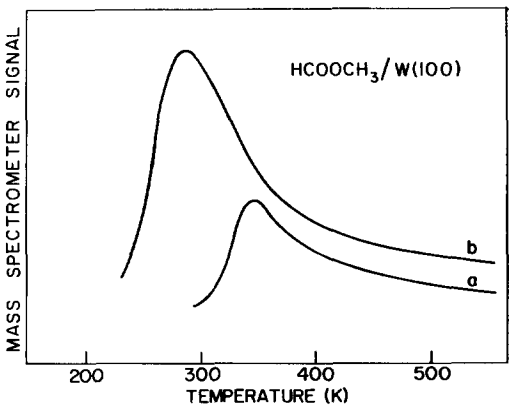

FIG. 2. Desorption of $HCOOCH_3$ from W(100). (a) T_a = 295 K; (b) T_a = 230 K.

W(100)–CO(β)

The decomposition of methyl formate on the W(100) surface was quite sensitive to the amount of CO(β) adsorbed on the surface before exposure to $HCOOCH_3$. When the surface was contaminated with small amounts of CO(β), an additional desorption peak for CH_3OH and H_2CO was observed near 400 K. When the W(100)–CO(β) surface was formed by saturation of the surface with CO(β) prior to adsorption of $HCOOCH_3$, the product peaks observed at 500 K on the clean W(100) surface disappeared, and CH_3OH and H_2CO were observed only at 408 K. Since the CO(β) states were saturated before adsorption of methyl formate, no additional CO(β) was formed by cracking $HCOOCH_3$ as was observed on the clean W(100) surface. The desorption spectra for unreacted $HCOOCH_3$, CO(β), and CO_2 were very similar to those observed on the initially clean W(100) surface; $HCOOCH_3$ adsorbed at 295 K, desorbed at 355 K, CO(β) at 381 K, and CO_2 above 560 K (see Fig. 3); H_2 desorbed at 408 K. Absolute coverages of the products are listed in Table 2. The peak temperatures for all of the products observed on the W(100)–CO(β) surface were coverage invariant, indicating that all of the products resulted from first-order rate processes. In addition, *no* CH_4 was formed on the W(100)–CO(β) surface.

W(100)–(5 × 1)C

The decomposition behavior of $HCOOCH_3$ on the W(100)–(5 × 1)C surface included features of the behavior observed on both the clean W(100) and W(100)–CO(β) surfaces as shown in Fig. 4. On the W(100)–CO(β) surface CH_3OH was produced only at 408 K; on the W(100) surface CH_3OH was produced only at 500 K; and on the W(100)–(5 × 1)C surface CH_3OH was produced at saturation coverage at both 408 and 470 K, with the peak at 470 K

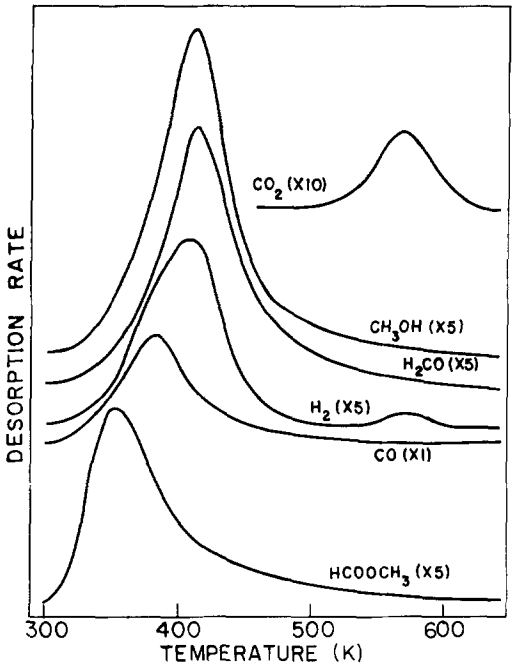

FIG. 3. Product desorption spectra for $HCOOCH_3$ adsorption on W(100)–CO(β): saturation exposure.

shifting to 500 K for low coverages. The complete product desorption spectrum for the decomposition of $HCOOCH_3$ on the W(100)–(5 × 1)C surface (Fig. 5) shows that the desorption spectra for the other products also resembled the sum of that observed on the W(100) and W(100)–CO(β) surfaces. As on the W(100) surface, the CH_3OH, H_2CO, CH_4, H_2, and CO products were evolved from an intermediate species of stoichiometry $CH_{4.5}O$ near 500 K. On the W(100)–(5 × 1)C surface these products were evolved simultaneously at 470 K for saturation coverages, and all shifted to 500 K as the coverage was reduced. The reaction order for the CH_4 product on the W(100)–(5 × 1)C surface was determined by isotherm–isostere methods (*18*). As shown in Fig. 6, the apparent reaction order was near one for low coverages, and increased toward two as the coverage was increased. Similar behavior was observed for the reactions of CH_3OH and H_2CO to form CH_4 on the same surface (*14, 15*). The shift in apparent reaction order has been attributed to repulsive interactions between adsorbed species, which result in a coverage-dependent activation energy (*18, 19*).

As on the CO(β)-saturated surface, no $HCOOCH_3$ was cracked to form CO(β), so that the stoichiometry of $HCOOCH_3$ with respect to carbon and hydrogen was recovered in the desorbing products (see Table 2). Small amounts of adsorbed oxygen (3% of a monolayer as determined by AES) were observed on the surface after each experiment. By addition of the coverage of O(a) from AES measurements to the coverages determined by thermal desorption of the remaining products, it was determined that the overall stoichiometry of the reacting $HCOOCH_3$ was recovered for reactions on the W(100)–(5 × 1)C surface.

DISCUSSION

The decomposition of methyl formate on the W(100), W(100)–(5 × 1)C, and W(100)–CO(β) surfaces closely resembled the decomposition of methanol (*14*) and formaldehyde (*15*) on those surfaces. The following common features were observed for all three reactants:

(1) The W(100) surface initially dissociated adsorbing species into CO(β) and hydrogen. Other products were observed only as the CO(β) states neared saturation. Further exposure to the adsorbing species re-

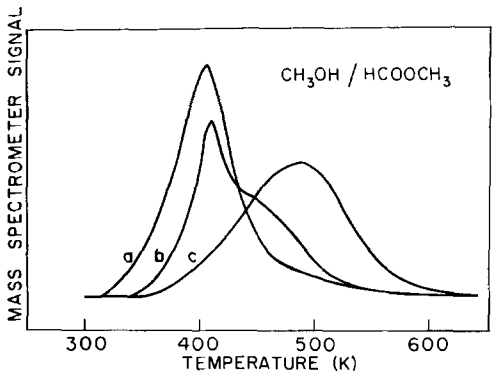

FIG. 4. CH_3OH desorption following $HCOOCH_3$ adsorption. (a) On W(100–CO(β); (b) on W(100)–(5 × 1)C; (c) on W(100).

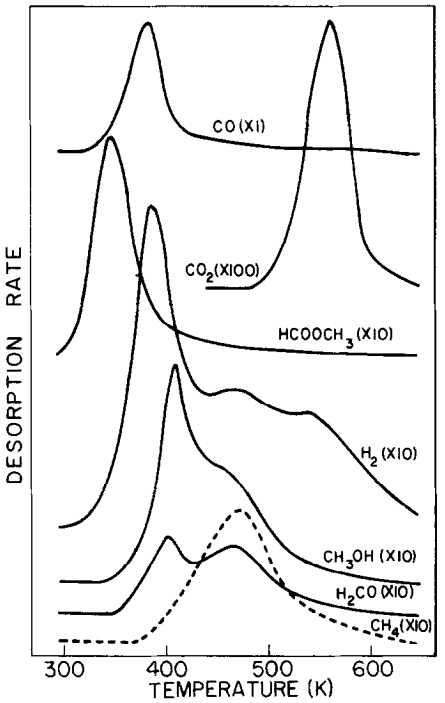

FIG. 5. Product desorption spectra for $HCOOCH_3$ adsorption on W(100)–(5 × 1)C: saturation exposure.

sulted in the displacement of some hydrogen from the surface, so that the overall stoichiometry of the parent molecule was not recovered in the products formed on this surface.

(2) The effect of presaturation by CO(β) and of deposition of surface carbon to form the (5 × 1) structure was to passivate the surface with respect to the dissociation of the parent molecule into CO(β) and hydrogen. This passivation of the surface reactivity allowed the production of various hydrocarbon species.

(3) Methane was produced on both the W(100) and W(100)–(5 × 1)C surfaces upon the decomposition of a surface complex above 470 K. The surface complexes resulting from the adsorption of different parent molecules all exhibited a stoichiometric excess of hydrogen relative to CH_3O, although the selectivity toward various hydrocarbons produced from this complex depended upon the nature of the parent molecule.

(4) No hydrocarbon products were observed on the W(100)–CO(β) surface above 408 K, and no CH_4 was produced on this surface.

These common observations suggested that the formation of various products from the different reactants adsorbed involved nearly identical mechanistic steps.

Worley and Yates (*13*) previously examined the decomposition of $HCOOCH_3$ on the W(100) surface. The results reported here help to clarify their results further. They reported desorption of hydrocarbon species from an adsorbed layer of $HCOOCH_3$ in a two-peak spectrum, with peaks located near 400 and 500 K for heating rates of 30 K/sec. The high-temperature peak was observed in this study on the W(100) surface; however, the low-temperature peak must be attributed to patches of W(100)–CO(β) surface as it was found to be reproducible only if CO(β) was adsorbed on the surface before exposure to $HCOOCH_3$. Further, the magnitude of the low-temperature peak, observed at 408 K, was found to be sensitive to the level of CO(β) preadsorbed on the surface. Fluctuations in the

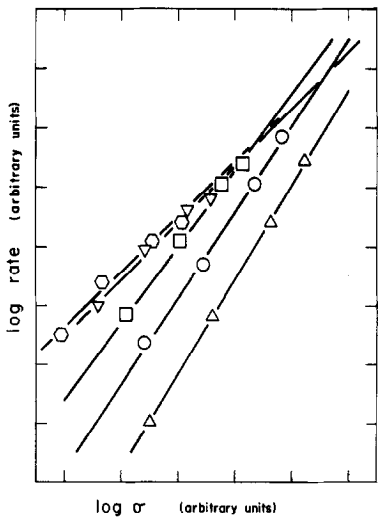

FIG. 6. CH_4 desorption following $HCOOCH_3$ adsorption on W(100)–(5 × 1)C: log rate vs log coverage. (△) T = 440 K, slope = 1.6; (○) T = 470 K, slope = 1.5; (□) T = 500 K, slope = 1.3; (▽) T = 525 K, slope = 1.0; (○) T = 547 K, slope = 0.9.

level of this contamination could easily lead to the discrepancies in the apparent product cracking patterns described by Worley and Yates (*13*). The results of the work reported here also showed that methyl formate desorbed from this surface at 355 K when adsorbed at room temperature, with a distribution of binding states accessible only when the adsorption temperature was reduced. The various reaction products resulted from the dissociative adsorption of $HCOOCH_3$ and did not involve these low-temperature binding states. Thus it is unlikely that $HCOOCH_3$ can act as a true intermediate in the formation of various hydrocarbon species from H_2CO at temperatures above 400 K, although the CO_2 produced was, indeed, the result of the decomposition of a stable surface formate intermediate.

A comparison of the decomposition of $HCOOCH_3$ on the W(100) and W(100)–CO(β) surfaces suggests that the hydrocarbon products evolved from these two surfaces were produced by different reaction pathways. On the initially clean W(100) surface, hydrocarbons, including CH_4, were produced from $HCOOCH_3$ only at 500 K. On the W(100)–CO(β) surface, hydrocarbons were produced only at 408 K, and no CH_4 was produced. Since the initial reaction on the W(100) surface was to crack $HCOOCH_3$ into CO(β) and H(a), the most significant difference between these two surfaces was that excess H(a) was present when reaction intermediates formed on the W(100) surface, whereas it was absent on the W(100)–CO(β) surface. In spite of the displacement of large quantities of hydrogen from the surface during the adsorption of $HCOOCH_3$, the reaction pathway on the W(100) surface was quite sensitive to the amount of CO preadsorbed, indicating that two types of sites were formed on this surface: "Hydrogen-containing" sites formed by cracking species such as $HCOOCH_3$, CH_3OH, or H_2CO and "hydrogen-deficient" sites formed by prior adsorption of CO into the β states. Yates and Madey (*8*) have shown that if H_2 is adsorbed on a W(100) surface, subsequent adsorption of CO at 100 K does not result in substantial displacement of the hydrogen, although the peak temperature of H_2 desorption is reduced. If, however, CO is adsorbed first, it is difficult to subsequently adsorb hydrogen. Thus it appears that the CO(β) and H(a) formed by cracking hydrocarbon species is equivalent to that formed by preadsorbing or co-adsorbing hydrogen with CO, and that only surface sites which are saturated with dissociated CO by this process retain the hydrogen which subsequently interacts with adsorbing $HCOOCH_3$. Since the decomposition behavior of $HCOOCH_3$ observed here closely resembled that of CH_3OH (*14*), it is proposed that this interaction of $HCOOCH_3$ with adsorbed hydrogen on the surface produced adsorbed methoxy groups (CH_3O). This mechanism is consistent with the observed stoichiometry of the products which desorbed from the W(100) surface following exposure to $HCOOCH_3$. Some of the CH_3O groups decomposed to liberate CO and H_2 at 390 K, with the remaining CH_3O groups "trapping" hydrogen into the complex structures of stoichiometric composition $CH_{4.5}O$ which decomposed at 500 K. This behavior is best illustrated by the evolution of the H_2 product desorption spectrum as a function of coverage, shown in Fig. 7.

The H_2 product desorption spectrum shown in Fig. 7 proceeded through three distinct stages as the coverage of $HCOOCH_3$ was increased to the saturation level. The first stage was characterized by a downward shift in peak temperature shown by curves a, b, and c. At these coverages, $HCOOCH_3$ was cracked completely into CO(β) and H(a). Yates and Madey (*8*) demonstrated a similar downward shift of the $H_2(\beta_2)$ peak with increased exposure to CO for sequential adsorption of H_2 and CO. As the exposure to $HCOOCH_3$ was increased further, an additional H_2 peak was observed at 390 K (curve d) which became

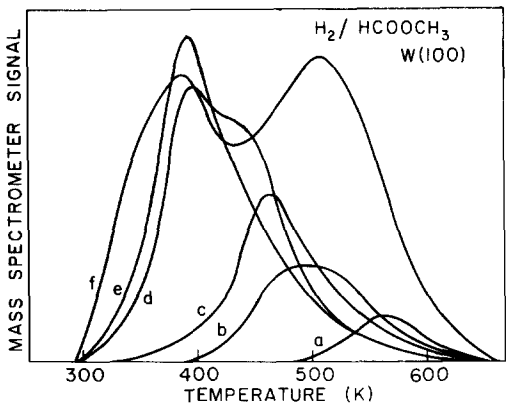

FIG. 7. H_2 desorption following $HCOOCH_3$ adsorption on W(100): coverage variation. (a) 3% of saturation exposure; (b) 6% of saturation exposure; (c) 12.5% of saturation exposure; (d) 25% of saturation exposure; (e) 50% of saturation exposure; (f) saturation exposure.

dominant with the disappearance of hydrogen from the β_2 state (curve e). As CO was also evolved at 390 K, it is suggested that CH_3O groups were first stabilized on the surface at exposures such as correspond to curve d, and decomposed at 390 K to yield CO and H_2. Further, at this exposure, the CO(β) states were very nearly saturated, as evidenced by the production of undissociated CO among the products and by the fact that slight increases in the exposure to $HCOOCH_3$ resulted in complete displacement of hydrogen from the β_2 state (curve e). At saturation coverage of $HCOOCH_3$, some of the hydrogen produced at 390 K reacted to stabilize the remaining CH_3O groups into a stable surface complex. Thus at saturation coverage, the H_2 desorption spectrum (curve f) showed peaks at both 390 and 500 K, resulting from the decomposition of CH_3O groups and of the surface complex, respectively. Additional products which resulted from the decomposition of the surface complex were CH_3OH, H_2CO, CH_4, and CO. Small amounts of CO_2 were observed at 595 K which were attributed to an HCOO intermediate, as CO_2 was produced from HCOOH at the same temperature (*20*). These formate species probably resulted from the oxidation of H_2CO by adsorbed oxygen formed with the formation of CH_4.

The decomposition of $HCOOCH_3$ on the W(100)–CO(β) surface proceeded by a different reaction pathway than on the clean W(100) surface. As there was no cracking of the parent molecule to CO(β) and H(a), there was no adsorbed hydrogen present on the W(100)–CO(β) surface with which the adsorbing $HCOOCH_3$ could interact. Rather, $HCOOCH_3$ dissociated to form HCO(a) and CH_3O(a). The subsequent decomposition of HCO(a) species yielded CO(β) and H(a) at 381 K. Decomposition of the CH_3O(a) species yielded CH_3OH, H_2CO, and H_2 at 408 K, with the evolution of H_2 characterized by a somewhat wider peak which included the hydrogen produced from both intermediate species. As on the W(100) surface, small amounts of CO_2 were also evolved on the W(100)–CO(β) surface above 560 K, which again appear to have been evolved from a formate intermediate.

It should be noted that due to the small separation of the decomposition temperatures of the HCO and CH_3O intermediate species, it was not possible to separate the decomposition into distinct regimes, with clearly defined sets of adsorbed species in each regime. Rather, the decompositions of the HCO(a) and CH_3O(a) species took place over ranges of temperature which overlapped, so that all intermediate and product species observed must be considered to have been present over the temperature range from 380 to 408 K. The effect of these overlapping decompositions was to change the decomposition selectivity for the CH_3O intermediate, as well as the desorption spectrum for H_2. For example, when CH_3OD was adsorbed on the W(100)–CO(β) surface, the decomposition of the CH_3O intermediate yielded CO as well as CH_3OH and H_2CO (*14*). When $HCOOCH_3$ was adsorbed on the surface, the production of CO from HCO effectively blocked the complete dissociation of the CH_3O intermediate to form CO. Likewise, although

the H_2 desorption spectrum exhibited a maximum at 408 K, this peak was wider than those of CH_3OH and H_2CO which occurred at the same temperature due to the evolution of hydrogen from the decomposition of the HCO intermediate at slightly lower temperature. Thus the reaction and desorption characteristics of surface species may be affected by the presence of other species.

With the exception of the initial formation of CO(β) from $HCOOCH_3$ on the W(100) surface, all of the steps of the mechanism proposed for the decomposition of methyl formate took place on at least two of the three surfaces examined. The complete mechanism for the decomposition of methyl formate, as well as the surface upon which each step occurs, are listed in Table 3. The decomposition behavior observed on the W(100)–(5 × 1)C surface was essentially the sum of that observed on the other two surfaces, and common intermediate species and reaction steps have therefore been proposed. It should be noted, however, that the product selectivity was dependent upon the surface involved, and common reaction steps do not imply common selectivity nor common rate parameters. These selectivity differences may be attributed to the geometric and electronic characteristics of the various surfaces. For example, although the same intermediate complex, designated *Y*, of stoichiometric

TABLE 3

Mechanism of $HCOOCH_3$ Decomposition[a]

Step	*T* (K)		Surface upon which step occurs		
			W(100)	W(100)–CO(β)	W(100)–(5 × 1)C
1	ads 295	$HCOOCH_3(g) \longrightarrow 2CO(\beta) + 4H(a)$	X		
2	ads 295	$HCOOCH_3(g) \longrightarrow HCO(a) + CH_3O(a)$		X	X
3	ads 295	$HCOOCH_3(g) + H(a) \rightarrow H_2(g) + CO(\beta) + CH_3O(a)$	X		
4	ads 295	$2H(a) \longrightarrow H_2(g)$	X		
5	ads 295	$HCOOCH_3(g) \longrightarrow HCOOCH_3(a)$	X	X	X
6	355	$HCOOCH_3(g) \longrightarrow HCOOCH_3(g)$	X	X	X
7	380–390	$HCO(a) \longrightarrow H(a) + CO(g)$		X	X
8	380–390	$CH_3O(a) \longrightarrow CO(g) + 3H(a)$	X		X
9	380–390	$CH_3O(a) + H(a) \longrightarrow Y$	X		X
10	380–390	$2H(a) \longrightarrow H_2(g)$	X	X	X
11	408	$CH_3O(a) \longrightarrow H_2CO(a) + H(a)$		X	X
12	408	$CH_3O(a) + H(a) \longrightarrow CH_3OH(g)$		X	X
13	408	$H_2CO(a) + O(a) \longrightarrow HCOO(a) + H(a)$		X	X
14	408	$H_2CO(a) \longrightarrow H_2CO(g)$		X	X
15	408	$2H(a) \longrightarrow H_2(g)$		X	X
16	471–500	$Y \longrightarrow CH_3OH(g) + CH_4(g) + CO(g) + H_2CO(a) + H(a) + O(a)$	X		X
17	471–500	$H_2CO(a) + O(a) \longrightarrow HCOO(a) + H(a)$	X		X
18	471–500	$H_2CO(a) \longrightarrow H_2CO(g)$	X		X
19	471–500	$2H(a) + O(a) \longrightarrow H_2O(g)$	X		X
20	471–500	$2H(a) \longrightarrow H_2(g)$	X		X
21	550	$HCOO(a) \longrightarrow CO_2(g) + H(a)$	X	X	X
22	550	$2H(a) \longrightarrow H_2(g)$	X	X	X

[a] *Y* is the proposed intermediate of stoichiometric composition $CH_{4.5}O$.

composition $CH_{4.5}O$ was proposed on both the W(100) and W(100)–(5 × 1)C surfaces for the production of hydrocarbons, including methane, above 470 K, the product selectivity and decomposition behavior of this intermediate differed on the two surfaces. The W(100)–(5 × 1)C surface was more selective for the formation of CH_4 and probably involved repulsive interactions as evidenced by the coverage-dependent activation energy for the decomposition of the complex as previously mentioned. These two effects may be explained by the geometries of the surfaces involved. The W(100)–(5 × 1)C surface has hexagonal symmetry (*16*) and may be expected to result in closer packing of the component species in the complex than the W(100) surface, which has square symmetry. Closer packing would be expected to result in stronger interaction of the component species as observed on the W(100)–(5 × 1)C surface.

The most likely candidate for the intermediate species, *Y*, is a complex structure of CH_3O groups, stabilized by excess hydrogen to yield the observed stoichiometry $CH_{4.5}O$. The formation of CH_4, CH_3OH, H_2CO, and H_2 above 470 K on the W(100) and W(100)–(5 × 1)C surfaces exhibits common energetics and thus implies that these species are formed from a common intermediate on each surface. As absorbed hydrogen is not stable on either surface at these temperatures, a hydrogen-stabilizing interaction within the complex intermediate, *Y*, is necessary in order to explain the observed stoichiometry. Other reaction pathways for formation of CH_4 such as hydrogenation of surface carbon do not appear to be important in the present case: such pathways can explain neither the formation of H_2CO and CH_3OH which accompanies CH_4 formation, nor the production of CH_4 on the clean W(100) surface. In addition previous studies (*16, 20*) have demonstrated that carbon on the W(100) surface cannot be hydrogenated either by adsorption of hydrogen at 300 K or the release of hydrogen by reaction at 600 K.

Thus it may be concluded that the interaction of adsorbed methoxy species with surface hydrogen was responsible for the production of the stable surface intermediate of stoichiometry $CH_{4.5}O$. The decompositions of both $HCOOCH_3$ and CH_3OD (*14*) demonstrated that CH_3O groups which are not stabilized by surface hydrogen (e.g., as on the W(100)–CO(β) surface) decompose below 410 K, and do not lead to the production of CH_4. While the mechanism of the stabilizing interaction remains unresolved, it is clear that the stabilization of CH_3O(a) by surface hydrogen is crucial in the production of methane and other hydrocarbons above 470 K on both the W(100) and W(100)–(5 × 1)C surfaces, and that $HCOOCH_3$ does not act as the intermediate in this process.

ACKNOWLEDGMENTS

The authors gratefully acknowledge the support of the ACS Petroleum Research Fund and the NSF–MRL Program through the Center for Materials Research at Stanford University in conducting this research. One of us (M.A.B.) is also grateful for the award of an NSF graduate fellowship.

REFERENCES

1. Swanson, L. W., and Gomer, R., *J. Chem. Phys.* **39,** 2513 (1963).
2. Yates, J. T., Jr., and King, D. A., *Surface Sci.* **30,** 601 (1972).
3. Goymour, C. G., and King, D. A., *J. Chem. Soc., Faraday Trans. 1* **69,** 736, 749 (1973).
4. Madey, T. E., and Yates, J. T., Jr., Colloque International sur la Structure et les Proprietes des Surfaces des Solides, CNRS, Paris (1969).
5. Tamm, P. W., and Schmidt, L. W., *J. Chem. Phys.* **51,** 5352 (1969).
6. Estrup, P. J., and Anderson, J., *J. Chem. Phys.* **45,** 2254 (1966).
7. Jaeger, R., and Menzel, D., *Surface Sci.* **63,** 232 (1977).
8. Yates, J. T., Jr., and Madey, T. E., *J. Chem. Phys.* **54,** 4969 (1971).
9. Vorburger, T. W., Sandstrom, D. R., and Waclawski, B. J., *Surface Sci.* **60,** 211 (1976).
10. Froitzheim, H., Ibach, H., and Lehwald, S., *Surface Sci.* **63,** 56 (1977).
11. Benziger, J. B., and Madix, R. J., *Surface Sci.* **77,** 1379 (1978).
12. Yates, J. T., Jr., Madey, T. E., and Dresser, M. J., *J. Catal.* **30,** 260 (1973).

13. Worley, S. D., and Yates, J. T., Jr., *J. Catal.* **48,** 395 (1977).
14. Ko, E. I., Benziger, J. B., and Madix, R. J., to be published.
15. Benziger, J. B., Ko, E. I., and Madix, R. J., to be published.
16. Benziger, J. B., Ko, E. I., and Madix, R. J., *J. Catal.* **54,** 414 (1978).
17. Debe, M. K., and King, D. A., *J. Phys. C* **10,** L303 (1977). *Phys. Rev. Lett.* **39,** 708 (1977).
18. Falconer, J. L., and Madix, R. J., *J. Catal.* **48,** 262 (1977).
19. Benziger, J. B., to be published.
20. Ko, E. I., Benziger, J. B., and Madix, R. J., *J. Catal.* **58,** 149 (1979).